THE JOURNAL OF BIOLOGICAL CHEMISTRY VOL. 284, NO. 15, pp. 10174–10180, April 10, 2009

Crystal Structure of a Two-domain Multicopper Oxidase

IMPLICATIONS FOR THE EVOLUTION OF MULTICOPPER BLUE PROTEINS[*S]

Received for publication, January 9, 2009, and in revised form, February 6, 2009 Published, JBC Papers in Press, February 17, 2009, DOI 10.1074/jbc.M900179200

Thomas J. Lawton[‡], Luis A. Sayavedra-Soto[§], Daniel J. Arp[§], and Amy C. Rosenzweig[‡1]

From the [‡]Departments of Biochemistry, Molecular Biology, and Cell Biology and of Chemistry, Northwestern University, Evanston, Illinois 60208 and the [§]Department of Botany and Plant Pathology, Oregon State University, Corvallis, Oregon 97331

The two-domain multicopper oxidases are proposed to be key intermediates in the evolution of three-domain multicopper oxidases. A number of two-domain multicopper oxidases have been identified from genome sequences and are classified as type A, type B, or type C on the basis of the predicted location of the type 1 copper center. The crystal structure of blue copper oxidase, a type C two-domain multicopper oxidase from *Nitrosomonas europaea,* has been determined to 1.9 Å resolution. Blue copper oxidase is a trimer, of which each subunit comprises two cupredoxin domains. Each subunit houses a type 1 copper site in domain 1 and a type 2/type 3 trinuclear copper cluster at the subunit-subunit interface. The coordination geometry at the trinuclear copper site is consistent with reduction of the copper ions. Although the overall architecture of blue copper oxidase is similar to nitrite reductases, detailed structural alignments show that the fold and domain orientation more closely resemble the three-domain multicopper oxidases. These observations have important implications for the evolution of nitrite reductases and multicopper oxidases.

Multicopper oxidases (MCOs)[2] are a widely distributed class of enzymes with diverse functions ranging from copper and iron metabolism to polyphenol oxidation. MCOs contain four copper ions arranged in two sites: a blue type 1 mononuclear copper center (T1) and a trinuclear copper cluster (T2/T3) consisting of a normal type 2 copper center (T2) and dinuclear type 3 (T3) center (1–3). Substrate oxidation is coupled to reduction of dioxygen to water via electron transfer from the T1 site to the T2/T3 cluster where dioxygen binds (4, 5). Because of structural similarities, MCOs are often grouped with copper nitrite reductases (NIRs), which contain both T1 and T2 sites (6), and are collectively referred to as multicopper blue proteins (MCBPs) (7). MCOs are composed of multiple cupredoxin domains, and both three-domain and six-domain variants have been studied. Three-domain MCOs (3dMCOs) include ascorbate oxidase, laccases, CueO, and Fet3. In these proteins, the T1 site is located in the C-terminal cupredoxin domain, and the T2/T3 cluster is located at the interface between domains 1 and 3 (8, 9). Ceruloplasmin is a six-domain MCO that houses T1 sites in domains 2, 4, and 6 and a T2/T3 cluster between domains 1 and 6 (10).

Because of the prevalence of cupredoxin domains, blue copper proteins, and MCOs in nature, understanding their origins has the potential for addressing important questions about the evolution of protein size, function, structure, and complexity (11). Several models for the evolution of three- and six-domain MCOs have been proposed. In these models, the key evolutionary intermediates are two-domain ancestral MCOs (7, 11, 12). The two-domain MCOs (2dMCOs) are hypothesized to result from a single domain duplication event and have architectures resembling the homotrimeric two-domain NIRs. NIRs contain a T1 site in each domain 1 and a T2 site at the intersubunit interfaces between domains 1 and 2 (7, 11–13). On the basis of genome sequence analysis, three types of two-domain MCOs (2dMCOs) have been predicted and are classified according to the proposed location of the T1 copper sites (7) (Fig. 1). The type A 2dMCOs contain a T1 site in each domain, whereas the type B and type C 2dMCOs contain a single T1 site in the second or first cupredoxin domains, respectively. The latter two types are postulated to have evolved from the type A 2dMCOS.

Despite the recent identification of genes encoding 2dMCOs (7), biochemical and structural characterization of these proteins has been limited. The first 2dMCO isolated was blue copper oxidase (BCO, encoded by NE0925 (14)) from *Nitrosomonas europaea*, originally described as a *p*-phenylenediamine oxidase (15) and identified as a type C 2dMCO almost 20 years later (7, 13). Of all the 2dMCOs identified by Nakamura *et al.* (7, 13), BCO was predicted to be the most similar to NIRs. In addition to laccase-like activity, BCO was found to oxidize the ferrous heme groups in hydroxylamine oxidoreductase and cytochrome *c*-554. Nitrite reductase activity was also observed using reduced cytochrome *c*-552 as an electron donor (15). Beyond BCO, three 2dMCOs from *Streptomyces* have been characterized biochemically: EpoA from *Streptomyces griseus* (16), SLAC from *Streptomyces coelicolor* (17), and a halotoler-

* This work was supported, in whole or in part, by National Institutes of Health Grant GM070473 (to A. C. R.). This work was also supported by a grant from the Oregon Agricultural Experimental Station (to O. S. U.).

The atomic coordinates and structure factors (code 3G5W) have been deposited in the Protein Data Bank, Research Collaboratory for Structural Bioinformatics, Rutgers University, New Brunswick, NJ (http://www.rcsb.org/).

[S] The on-line version of this article (available at http://www.jbc.org) contains two supplemental figures and three supplemental tables.

[1] To whom correspondence should be addressed. Tel.: 847-467-5301; Fax: 847-467-6489; E-mail: amyr@northwestern.edu.

[2] The abbreviations used are: MCO, multicopper oxidase; 3dMCO, three-domain multicopper oxidase; 2dMCO, two-domain multicopper oxidase; MCBP, multicopper blue protein; BCO, blue copper oxidase; T1, type 1 copper site; T2, type 2 copper site; T3, type 3 copper site; NIR, nitrite reductase; AfNIR, NIR from *Alcaligenes faecalis*; AxNIR, NIR from *Alcaligenes xylosoxidans*; AniA, NIR from *Neisseria gonorrhoeae*; RIL, *Rigidoporus lignosus* laccase; SLAC, small laccase from *Streptomyces coelicolor*; r.m.s.d., root-mean-square deviation; PDB, Protein Data Bank; ABTS, 2,2′-azinobis(3-ethylbenzthiazoline-6-sulfonate); Pipes, 1,4-piperazinediethanesulfonic acid.

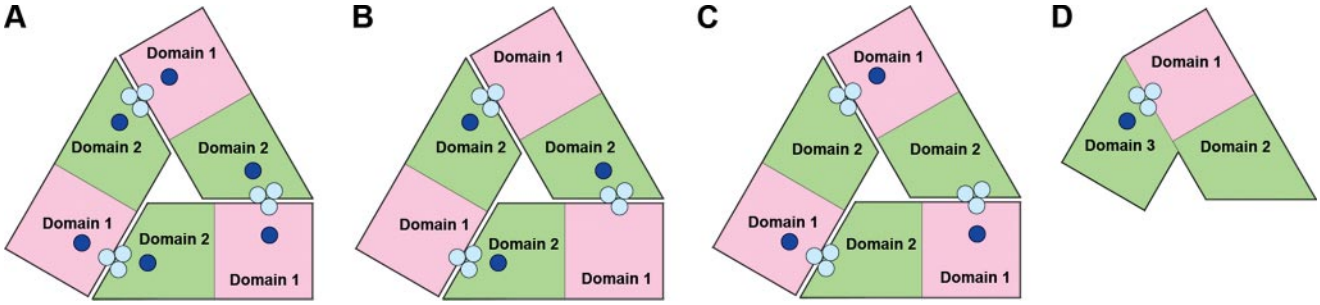

FIGURE 1. **Schematic diagram of the domain organization and copper sites of MCOs.** T1 sites are shown as *dark blue circles*, and T2/T3 clusters are shown as *light blue circles*. *A*, type A 2dMCO. *B*, type B 2dMCO. *C*, type C 2dMCO. Domain 1 is shown in *pink*, and domain 2 is shown in *green*. *D*, 3dMCO. Domain 1 is shown in *pink*, and domains 2 and 3 are shown in *green*.

ant-alkaline laccase from *Streptomyces psammoticus* (18). The amino acid sequences for EpoA and SLAC are known, and sequence alignments indicate they are type B 2dMCOs (13). Although the *S. psammoticus* laccase was not specifically identified as a 2dMCO, its small molecular mass of 43 kDa is suggestive of a 2dMCO. The physiological role of the 2dMCOs is not clear, but the biochemical data indicate substrate specificities similar to three-domain laccases (15–18). The crystal structure of the type B 2dMCO SLAC was recently determined to 2.7 Å resolution and revealed a homotrimer with an overall architecture similar to NIRs (19). To further understand 2dMCOs and the relationships between NIRs and MCOs, we have determined the crystal structure of a type C 2dMCO, BCO from *N. europaea*, to 1.9 Å resolution.

MATERIALS AND METHODS

Cell Growth—N. europaea cells were grown in batch cultures at 30 °C in the dark (20, 21). Cultures were grown in Erlenmeyer flasks (1.5 liters) and polypropylene carboys (9 liters) for 72 h on a rotary shaker (200 rpm) and used for inoculants. Each large scale cell culture (closed high density polyethylene dome tanks, 120-liter cultures) was inoculated with the contents of a carboy. The dome tanks were aerated for about 48 h with an oil-less diaphragm pump (3–5 liter/min) through coarse glass spargers to allow proper mixing. The large scale cell cultures were harvested at ~0.06 A_{600} using a tangential-flow system equipped with two ultrafiltration modules (Millipore, MA). The concentrated cells were then collected by centrifugation and resuspended with an equal volume of sodium phosphate buffer (50 mM NaH_2PO_4, 2 mM $MgCl_2$). This resuspension was flash-frozen in liquid nitrogen and stored at −80 °C until used.

BCO Purification and Activity—For protein isolation, *N. europaea* cells were sonicated and centrifuged for 30 min at 129,000 × *g*. Following a 40% $(NH_4)_2SO_4$ precipitation step, the supernatant was applied to a phenyl-Sepharose column (GE Life Sciences) equilibrated with 20 mM Tris·HCl (pH 8.0) and 1.7 M $(NH_4)_2SO_4$ and eluted with 20 mM Tris·HCl (pH 8.0). Fractions blue in color were concentrated using an Amicon centrifuge filter (50-kDa molecular mass cutoff, Millipore) and loaded onto a S-200 HiPrep® gel filtration column (GE Life Sciences) equilibrated with 20 mM Pipes (pH 6.8) and 20 mM NaCl. Oxidation of 2,2′-azinobis(3-ethylbenzthiazoline-6-sulfonate) (ABTS) by purified enzyme was measured on a Cary 500 spectrophotometer using 20 mM Pipes (pH 6.8), 1 mM ABTS, and 20 mM NaCl (22) at a final protein concentration of 0.275 mg/ml. From five replicates, BCO was found to oxidize ABTS at a rate of 105.1 ± 4.24 μmol·min^{-1} mg^{-1} protein. Protein concentration was measured as described previously (15).

Crystallization and Data Collection—Crystals of BCO were grown by sitting drop vapor diffusion at 4 °C using 100 mM Tris·HCL (pH 7.5), 4% glycerol, and 40% 2-methyl-2,4-pentane-diol as a reservoir solution. Protein samples (1 μl of 2.75 mg·ml^{-1} in 20 mM Pipes (pH 6.8), 20 mM NaCl) were mixed with 1 μl of reservoir solution. Crystals grew within 1 day to ~0.05 mm in the longest dimension and belong to the space group P1 with unit cell dimensions $a = 76.1$, $b = 76.3$, $c = 105.2$, $\alpha = 81.5$, $\beta = 73.4$, $\gamma = 61.8$. Crystals were cryoprotected using fresh reservoir solution and flash-frozen in liquid nitrogen. Data sets were collected at the Life Sciences Collaborative Access Team (LS-CAT) (sector 21) beamline ID-D and at the General Medicine and Cancer Institutes Collaborative Access Team (GM/CA-CAT) (sector 23) beamline ID-D at the Advanced Photon Source (APS), Argonne, IL using a Mar 300 CCD detector. Data sets were processed using the HKL2000 package (23) (Table 1).

Structure Determination and Refinement—The structure was solved using copper multiwavelength anomalous dispersion (Table 1). Using autoSHARP, all 24 copper sites were located, and density modification was performed using a solvent content of 47.2% (24). The initial model was built with Coot (25) using polyalanine chains generated automatically with ARP/wARP (26) and refined against 1.9 Å diffraction data with Refmac5 (27). Six-fold noncrystallographic symmetry was used in the early stages of refinement. Two homotrimers comprise the asymmetric unit. The final model (Table 1) consists of residues 44–361 for each of the six chains (A–F), 24 copper ions, 2,009 water molecules, and four glycerol molecules. The first 43 residues are predicted to be a periplasmic signal peptide, and the 2 C-terminal residues were not observed in the electron density. A Ramachandran plot calculated with PROCHECK (28) indicates that 100% of the residues are in the most favored and additionally allowed regions. Figures were generated with PyMOL (29).

Sequence and Structure Alignments—Sequence alignments (supplemental Fig. S1) were generated using the program T-Coffee (30, 31). The BCO coordinates were superposed onto coordinates of 13 other MCOs using the Secondary Structure Matching algorithm (32). The BCO model used for pairwise superposition onto 3dMCOs consisted of chain A

TABLE 1
Data collection and refinement statistics

	Native[a]	Low remote[b]	High remote[c]	Peak[b]
Data collection				
Wavelength (Å)	0.91933	1.3811	1.3189	1.3476
Resolution (Å)	1.9 (1.97–1.90)	2.51 (2.6–2.51)	2.39 (2.48–2.39)	2.52 (2.61–2.52)
R_{sym}[d,e]	0.083 (.342)	0.090 (.231)	0.186 (.404)	0.074 (.252)
I/σI	16.9 (4.8)	14.9 (4.0)	12.3 (3.3)	4.0 (1.9)
Completeness (%)	98.2 (98.2)	99.2 (75.2)	100 (98.8)	99.4 (78.8)
Redundancy	24.3 (2.6)	3.7 (3)	10.3 (5.4)	7.4 (5.5)
Refinement				
No. of reflections	145,469			
R_{work}[f]/R_{free}[g]	0.196/0.167			
Average *B*-factor	23.92			
r.m.s. deviations				
Bond lengths (Å)	0.008			
Bond angles (°)	1.157			

[a] Data from two different crystals were included.
[b] Data from one crystal were used.
[c] Data from three different crystals were included.
[d] $R_{sym} = \sum| I_{obs} - I_{av}|/\sum F_{obs}$, where the summation is over all reflections.
[e] Values in parentheses refer to the highest-resolution shell.
[f] $R_{work} = \sum|F_{obs} - F_{calc}|/\sum F_{obs}$
[g] For calculation of R_{free}, 5% of the reflections were reserved.

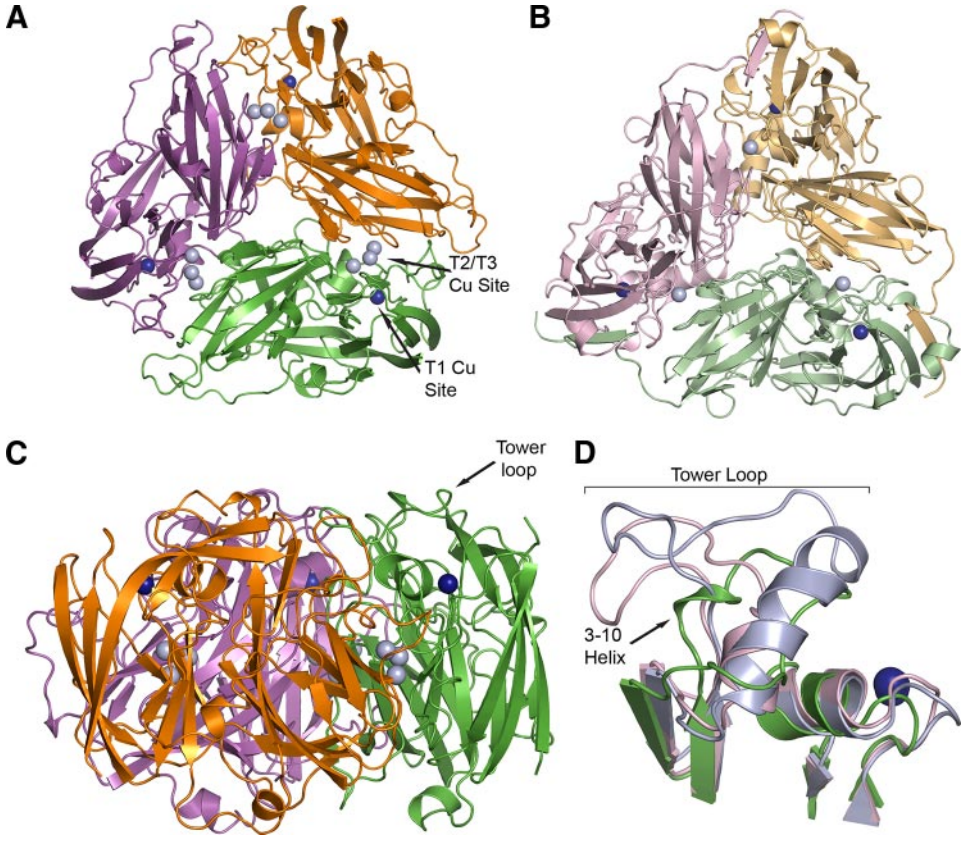

FIGURE 2. **Overall architecture of BCO and comparison with NIR.** T1 copper ions are shown as *dark blue spheres*, and T2/T3 copper ions are shown as *light blue spheres*. *A*, BCO viewed looking down the trimer 3-fold axis. The three subunits are shown in *green*, *orange*, and *dark pink*. *B*, AfNIR (PDB accession code 1AS7) viewed looking down the trimer 3-fold axis. The three subunits are shown in *light green*, *light orange*, and *light pink*. *C*, BCO viewed 90° from the orientation in *A*. The tower loop is indicated with a *black arrow*. *D*, superposition of the NIR tower loop with the corresponding region in BCO. AniA (PDB accession code 1KBW) is shown in *light pink*, AfNIR (PDB accession code 1AS7) is shown in *light blue*, and BCO is shown in *green*.

residues 44–318 and residues 179–318 from chain B. As a control, similar constructs of AniA and SLAC were superposed in the same fashion. BCO subunits were also pairwise-superposed onto subunits from five different NIRs. In cases in which the Secondary Structure Matching algorithm presented multiple solutions, the solution with the lowest r.m.s.d. and comparable %sse (percentage of secondary structure of query protein found in target protein) is reported in Table 2 and supplemental Table S2.

To evaluate the effect of lattice contacts on the tower loop regions, subunits with tower loops involved in crystal packing (chains A, B, D, E, and F) were superposed onto the tower loop of chain C, which is not involved in lattice formation. Crystal contacts using a 5 Å cut-off were identified using the CCP4 program CONTACT (33) and by visual inspection. Residues 189–208 from each subunit were superposed using the program TopMatch (34, 35). Tower loop superposition results can be found in supplemental Table S3.

RESULTS AND DISCUSSION

Overall Structure—BCO comprises a cylindrical homotrimer (Fig. 2, *A* and *C*). Each subunit consists of two cupredoxin domains (domain 1 and domain 2), and the overall architecture resembles that of NIRs (Fig. 2*B*). Although primary sequence alignments and three-dimensional superpositions show that the core domains of BCO are well conserved in NIRs (supplemental Fig. S1), there are several significant differences. First, the loop proximal to the T1 site is different. In NIRs, this solvent-exposed loop, referred to as the tower loop (36), acts as docking surface for proteinaceous electron donors (37–39). The NIR tower loop extends from the first β-strand domain 2 to an α-helix ranging

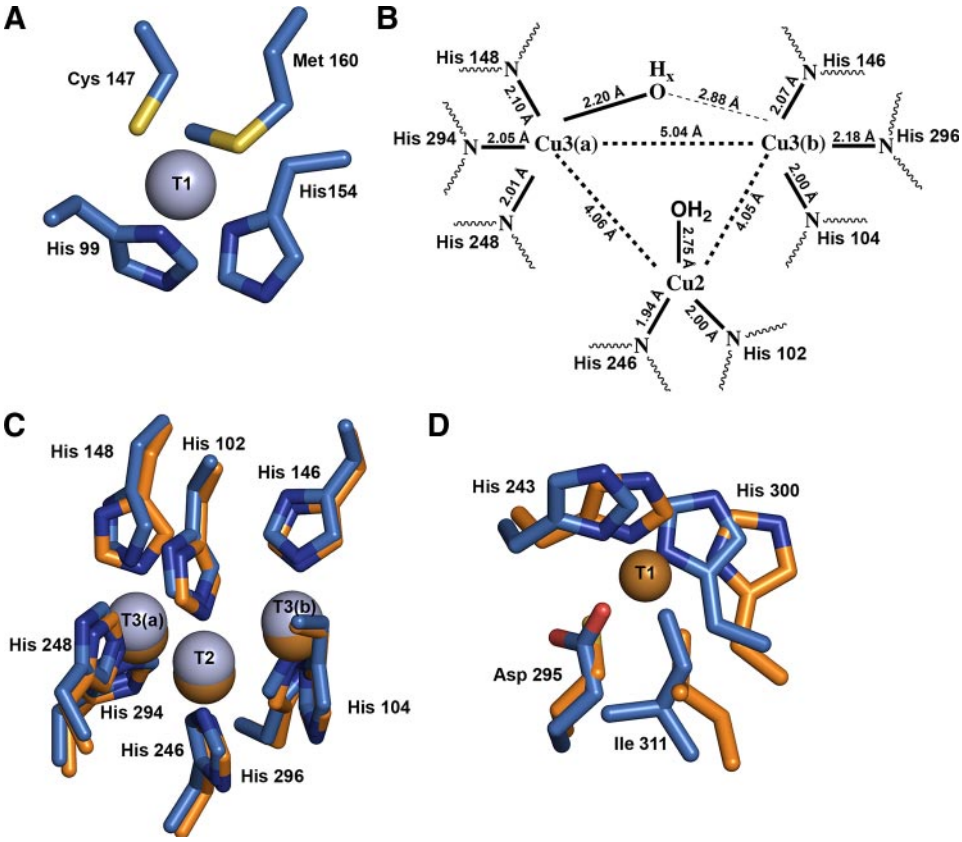

FIGURE 3. **The BCO metal centers.** *A*, the T1 site. *B*, a schematic diagram of the T2/T3 site. Metal ligand distances represent the average over six subunits in the crystallographic asymmetric unit. *C*, the T2/T3 site superposed on the T2/T3 site from RlL (PDB accession code 1V10). BCO is shown in *blue*, and RlL is shown in *orange*. *D*, superposition of the T1 site from RlL onto the corresponding region in BCO. BCO is shown in *blue*, and RlL is shown in *orange*.

in size from one-and-a-half turns to four turns. The corresponding region in BCO is 15 amino acids shorter than that in the NIRs from *Alcaligenes faecalis* (AfNIR) (40, 41) and *Alcaligenes xylosoxidans* (AxNIR) (42) and 8 amino acids shorter than that in AniA, a NIR from *Neisseria gonorrhoeae* (Fig. 2*D*) (43). Although AniA lacks part of the tower loop, the effect of the deletion is very different in BCO. In the BCO tower loop region, the first β-strand of the domain 2 is followed by a short 3_{10} helix that extends into a long loop. This loop is positioned similarly to the four-turn α-helix found in both AfNIR and AxNIR despite forming no secondary structure. The C terminus of the AniA tower loop retains some helical structure that aligns well with the C-terminal part of the AfNIR and AxNIR helices. However, the loop regions of AniA and BCO preceding this helix adopt different orientations than the loop regions in AfNIR and AxNIR (Fig. 2*D*). As a result of the modified tower loop region, the surface of the BCO trimer is much less contoured than those of NIRs. This difference likely explains the *in vitro* ability of BCO to accept electrons from proteinaceous donors of drastically different shapes and sizes (15). Interestingly, the tower loop region in the *N. europaea* NIR is also truncated (supplemental Fig. S1). It may be that NIR and BCO from *N. europaea* can accept electrons from similar protein donors.

It is important to note that five of the six tower loops in the asymmetric unit are involved in crystal contacts. Superposition of these tower loops with that from chain C, which is not involved in crystal lattice formation, gives r.m.s.d. values of ~0.1 Å (supplemental Table S3). Thus, crystal packing cannot account for all the observed conformational differences.

The second notable difference between BCO and NIRs is the position of the C terminus. In some NIR structures, the C-terminal extension stabilizes the trimer by forming a β-strand that interacts with the domain 1 β-sheet from an adjacent subunit (41, 44) (Fig. 2*B*). In BCO, the C terminus extends across the solvent-exposed side of domain 2, forming a short β-strand that interacts with domain 1 from the same subunit. The last 10 residues extend over the first two strands of domain 1 toward the T1 site.

The Copper Centers—Anomalous difference maps indicate that the BCO trimer contains 12 copper ions, arranged in three T1 sites, and three T2/T3 clusters. The T1 sites are located in domain 1 of each subunit and are ~13 Å from the nearest T2/T3 cluster. Although access to the BCO T1 site is more limited by the conformation of the tower loop region than in other MCOs, such as *Rigidoporus lignosus* laccase (RlL) (45), the BCO T1 site is still capable of accepting electrons from multiple proteinaceous and nonproteinaceous donors (15). The T2/T3 sites are positioned at the subunit-subunit interfaces, similar to the location of the T2 site in NIRs. By contrast, the T1 center in 3dMCOs is located in domain 3, and the T2/T3 site is located at the interface between domains 1 and 3. The BCO T1 sites are coordinated by His-99, His-154, and Cys-147 in trigonal planar geometry, as well as an axial methionine, Met-160 (Fig. 3*A*). The metal-ligand distances are similar to those of other T1 sites (supplemental Table S1).

The BCO T2/T3 sites are coordinated by 8 histidines, His-102, His-104, His-146, and His-148 from domain 1 and His-246, His-248, His-294, and His-296 from domain 2 of the adjacent subunit (Figs. 2*A* and 3, *B* and *C*). Similar to other MCOs (46), there are two solvent channels leading to the trinuclear copper cluster. Unlike SLAC, neither of these channels originate from the core of the trimer. The T2 copper ion is coordinated by His-102, His-146, and a solvent ligand. The T3 copper ions are ligated by 3 histidines each and a solvent ligand that is clearly coordinated to Cu3(a) but 2.7–3.0 Å from Cu3(b) (Fig. 3*D* and supplemental Table S1). Interestingly, the BCO T2/T3 copper ions are coordinated by seven δ nitrogen atoms and one ϵ nitrogen atom similar to most other 3dMCOs, whereas SLAC uses an all ϵ nitrogen ligation similar to ceruloplasmin (19).

The average Cu-Cu distances in BCO are 5.04, 4.05, and 4.04 Å (Fig. 3*B*). These distances are similar to those observed in the crystal structures of laccases from *R. lignosus* (RlL) (45), *Coriolus zonatus*, and *Cerrena maxima* (8, 47, 48), all of which have a solvent ligand coordinated to Cu3(a). A terminal solvent ligand to Cu3(a) is also observed in the structure of T2-depleted *Coprinus cinereus* laccase (49). The BCO Cu-Cu distances are also similar to those in the structure of reduced ascorbate oxidase (50). Superposition of BCO and RlL shows that not only are the metal distances similar, but the arrangement of histidine ligands at the T2/T3 site is well conserved (Fig. 3*C*). Although ascorbate oxidase was chemically reduced with dithionite, neither BCO nor RlL was treated with reductants. A probable explanation for the long Cu-Cu distances in RlL and BCO is photoreduction in the synchrotron beam. This phenomenon is well documented for metalloprotein crystals (51–53) and has been exploited to observe reduced intermediates in *Lentinus tigrinus* laccase (LtL) (54). Thus, the BCO T2/T3 clusters are likely at least partially reduced.

Although the BCO and laccase T2/T3 sites are structurally similar, formation of the trinuclear copper cluster in BCO is likely a more complex event. There is evidence that 3dMCOs sequentially reconstitute copper into the metal sites, loading the T1 site followed by the T2 and T3 sites (55, 56). In 3dMCOs, the T2/T3 cluster is located between domains 1 and 3. In BCO, the T2/T3 cluster is located at a subunit-subunit interface, so its formation must be preceded by oligomerization. In addition, a long linker connecting domain 2 to domain 3 in 3dMCOs may impart more flexibility to the T2/T3 binding site, allowing easier access for copper ions. This flexibility may also explain why the copper sites in 2dMCOs appear to be more stable once they are formed. Notably, the solvent channels leading to the T2/T3 sites in BCO contain four methionines, Met-106, Met-143, Met-292, and Met-312. These methionine residues might participate in recruiting copper for loading into the T2/T3 sites.

Implications for 2dMCO Structure and Function—BCO is a type C 2dMCO containing a single T1 site within domain 1 (Fig. 1). As of 2005, Nakamura and Go (13) identified 21 different 2dMCOs in genome databases: 3 type A, 17 type B, and 11 type C. On the basis of phylogenetic analysis, the type C 2dMCOs were further divided into three groups with BCO falling into its own class. Although no copper is present in domain 2 of BCO, superposition with the domain 3 RlL T1 site reveals that 2 histidines, His-243 and His-300, and a nearby hydrophobic residue, Ile-311, which occupies the axial position in laccases (8), are conserved (Fig. 3*D*). The RlL cysteine ligand is replaced by Asp-295 in BCO. Neither of the other two type C groups retain these 2 histidines and the hydrophobic residue in this position, suggesting that BCO is more closely related to the type A 2dMCOS, which have predicted T1 sites in both domains. In support of this notion, the type A 2dMCOs have a predicted tower loop region similar to that in BCO, whereas this region is missing in the other type C 2dMCOS (supplemental Fig. S1). These observations suggest that the ancestral type A 2dMCOs likely diverged at least two times to form modern type C 2dMCOs.

The physiological roles of the three classes of 2dMCO are not known. The tower loop in BCO and the type A family may facilitate electron transfer from proteinaceous donors to the domain 1 T1 site. The lack of a tower loop in the other type C 2dMCOs may indicate a different function. Interestingly, these proteins all have a conserved histidine at position 97 (BCO numbering) (supplemental Fig. S1). This residue, which is a leucine in BCO, is predicted to be close to the T1 site and could either bind substrates or participate in copper coordination. Of the 17 type B 2dMCOs catalogued by Nakamura and Go (13), 14 (not including EpoA and SLAC and NP_841583 from *N. europaea*) include methionine-rich C-terminal extensions and predicted methionine-rich surface patches, suggestive of a role in copper homeostasis (7), like the 3dMCO CueO (57). Because all the type B 2dMCOs except for EpoA, SLAC, and *N. europaea* NP_841583 contain predicted tower loops, the T1 site in domain 1 may have evolved away to avoid functioning as a terminal oxidase.

TABLE 2
Structural comparison of BCO with other MCBPs

Enzyme	r.m.s.d.	Organism	PDB
	Å		
3dMCOs			
Laccase	1.82	*Melanocarpus albomyces*	1GW0
Laccase	1.82	*Rigidoporus lignosus*	1V10
Lacasse	1.67	*Trametes trogii*	2HRG
Laccase	1.75	*Coriolus zonatus*	2HZH
Laccase	1.75	*Trametes versicolor*	1GYC
Laccase	1.82	*Cerrena maxima*	2H5U
Laccase	1.75	*Coriolopsis gallica*	2VDS
Laccase	1.79	*Lentinus tigrinus*	2QT6
Laccase	1.77	*Coprinus cinereus*	1HFU
CueO	1.91	*Escherichia coli*	2FQE
Fet3p	1.69	*Saccharomyces cerevisiae*	1ZPU
CotA (laccase)	1.85	*Bacillus subtilis*	1GSK
Ascorbate oxidase	1.43	*Cucurbita pepo var. melopepo*	1AOZ
Average	1.76		
NIRs			
AniA	2.02	*Neisseris gonorrhoeae*	1KBW
AxNIR	2.15	*Alcaligenes xylosoxidans*	1NDT
AfNIR	2.10	*Alcaligenes faecalis*	1AS7
AcNIR	2.05	*Achromobacter cycloclastes*	1NIC
RsNIR	2.06	*Rhodobacter sphaeroides*	1ZV2
Average	2.08		

BCO	Ascorbate oxidase		
	Domain 1	Domain 2	Domain 3
Individual domains			
Domain 1	1.00	2.00	1.78
Domain 2	1.82	1.44	1.46

Comparison with Other MCBPs and Evolutionary Implications—Structural comparison of BCO with other MCBPs reveals some striking similarities and differences. The two domains of the BCO subunit were superposed on five different NIRs with an average r.m.s.d. of 2.08 Å (Table 2 and supplemental Table S2). BCO and AniA (43) are quite similar with an r.m.s.d. of 2.02 Å. To facilitate comparison with 3dMCOs, a model containing one BCO subunit and domain 2 of an adjacent subunit was constructed (Fig. 4). An analogous model for AniA was also generated. BCO was superposed onto 13 different 3dMCOs with an average r.m.s.d. of 1.76 Å (Table 2). Ascorbate oxidase is the most similar with an r.m.s.d. of 1.43 Å. Superposition of AniA with the same 3dMCOs yields an average r.m.s.d. of 2.41 Å. The individual domains of BCO were also superposed onto single domains of AniA and several 3dMCOS (supplemental Table S2). The superpositions clearly show that

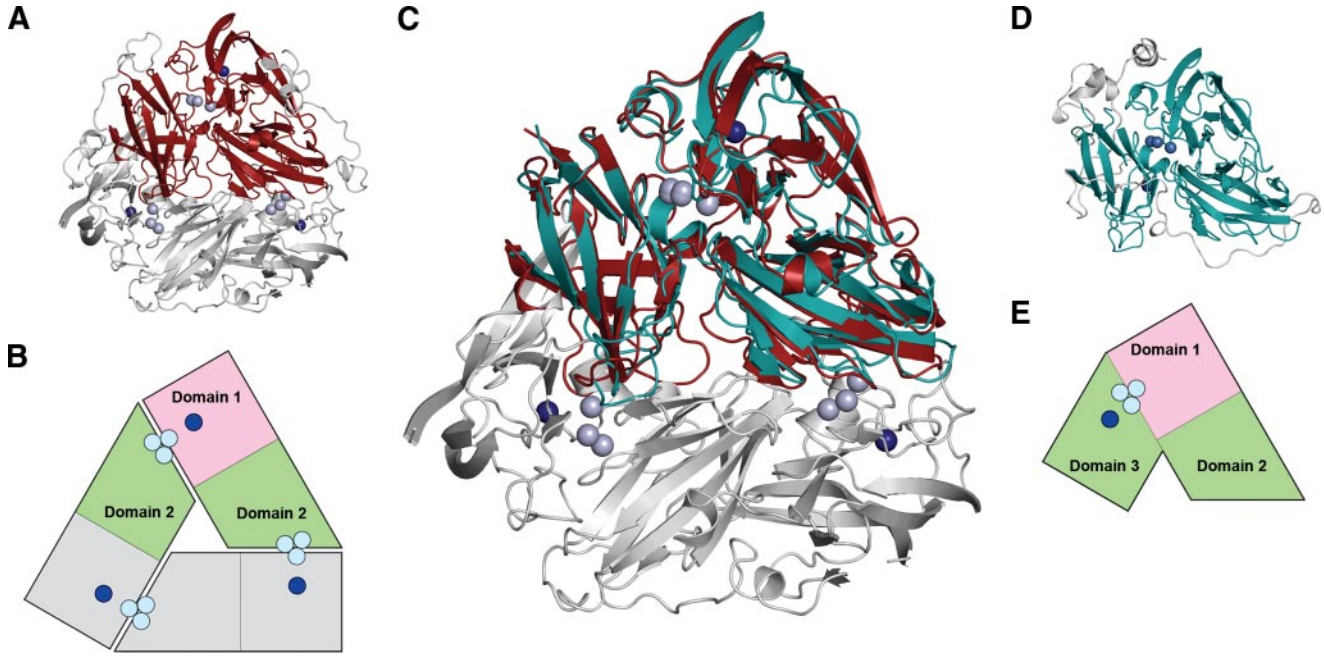

FIGURE 4. **Comparison of BCO with the 3dMCO RIL (PDB accession code 1V10).** Regions not used in the structural superposition and large unconserved loops are colored *gray*. *A*, BCO trimer with model used for structural comparison shown in *red*. *B*, a schematic diagram of BCO domain organization. The *green* and *pink domains* represent the red domains in *A*. *C*, superposition of RIL (*teal*) onto BCO (*red*). *D*, RIL with model used in superposition in *teal*. *E*, schematic diagram of RIL domain organization.

the overall folds and orientations of the cupredoxin domains are well conserved between BCO and the 3dMCOs (Fig. 4*C*) and match particularly well at the subunit interfaces. The r.m.s.d. values (Table 2) indicate that despite having the same overall architecture as NIRs, the orientation of the two domains in BCO is more similar to that in 3dMCOs.

In contrast, structural analysis of the type B 2dMCO SLAC indicated a closer similarity to AfNIR than to ascorbate oxidase and laccase from *Melanocarpus albomyces* (19). Our analysis with single subunits gives similar results (Table 2), but superposition of the individual SLAC domains indicates that SLAC domain 1 is more similar to domain 1 of the 3dMCOs than domain 1 of NIRs. Domain 2 of SLAC is more similar to domain 2 of NIRs than the second and third domains of 3dMCOs, however. It is therefore not surprising that BCO and SLAC superpose poorly with an r.m.s.d. of 2.07 Å.

Although the comparison of SLAC with NIRs might suggest a close evolutionary linkage (19), several structural features are consistent with a more distant relationship. The most obvious structural difference is the location of the T1 copper site. In SLAC, the T1 site is located in the second cupredoxin domain, whereas NIRs and BCO house the T1 site in their first cupredoxin domain. SLAC also lacks a tower loop, and the initial two β-strands in domain 1 are shorter than the corresponding strands in BCO and NIRs, resulting in a significantly different top surface. Beyond these major differences, SLAC contains two additional loops that are proposed to stabilize the trimer (19). Neither of these loops are present in NIRs or BCO.

Phylogenetic analysis conducted by Nakamura *et al.* (7, 13) indicated that BCO is the closest known 2dMCO relative to NIRs, leading to the hypothesis that NIRs might have evolved from a BCO-like type C 2dMCO via loss of the T3 site. However, they also noted that NIR could have descended directly from a common ancestor before the creation of the T2/T3 site. Given that superpositions show that the BCO domain arrangement is more similar to 3dMCOs than NIRs and evidence that BCO diverged recently from the type A 2dMCOs, we propose that NIRs evolved before MCOs acquired the trinuclear copper clusters. This scenario would also be more consistent with the evolutionary hypothesis for NIRs (58). Additional studies of 2dMCOs will be required to fully understand their physiological function and their role in MCBP evolution.

Acknowledgments—We thank the staffs at LS-CAT and GM/CA-CAT for assistance with data collection.

REFERENCES

1. Solomon, E. I., Sundaram, U. M., and Machonkin, T. E. (1996) *Chem. Rev.* **96,** 2563–2605
2. Messerschmidt, A. (ed) (1997) *Multi-Copper Oxidases*, World Scientific Publishing Company, Inc., Singapore
3. Messerschmidt, A., Huber, R., Poulos, T., and Wieghardt, K. (eds). (2006) *Handbook of Metalloproteins*, John Wiley & Sons, New York
4. Sakurai, T., and Kataoka, K. (2007) *CMLS Cell. Mol. Life Sci.* **64,** 2642–2656
5. Solomon, E. I., Augustine, A. J., and Yoon, J. (2008) *Dalton Trans.* 3921–3932
6. Suzuki, S., Kataoka, K., and Yamaguchi, K. (2000) *Acc. Chem. Res.* **33,** 728–735
7. Nakamura, K., Kawabata, T., Yura, K., and Go, N. (2003) *FEBS Lett.* **553,** 239–244
8. Zhukhlistova, N. E., Zhukova, Y. N., Lyashenko, A. V., Zaitsev, V. N., and Mikhailov, A. M. (2008) *Crystallogr. Rep.* **53,** 92–109
9. Taylor, A. B., Stoj, C. S., Ziegler, L., Kosman, D. J., and Hart, P. J. (2005) *Proc. Natl. Acad. Sci. U. S. A.* **102,** 15459–15464
10. Lindley, P. F., Card, G., Zaitseva, I., Zaitsev, V., Reinhammer, B., Selin-Lindgren, E., and Yoshida, K. (1997) *J. Biol. Inorg. Chem.* **2,** 454–463
11. Rydén, L. G., and Hunt, L. T. (1993) *J. Mol. Evol.* **36,** 41–66

12. Murphy, M. E., Lindley, P. F., and Adman, E. T. (1997) *Protein Sci.* **6,** 761–770
13. Nakamura, K., and Go, N. (2005) *CMLS Cell. Mol. Life Sci.* **62,** 2050–2066
14. Chain, P., Lamerdin, J., Larimer, F., Regala, W., Lao, V., Land, M., Hauser, L., Hooper, A., Klotz, M., Norton, J., Sayavedra-Soto, L., Arciero, D., Hommes, N., Whittaker, M., and Arp, D. (2003) *J. Bacteriol.* **185,** 2759–2773
15. DiSpirito, A. A., Taaffe, L. R., Lipscomb, J. D., and Hooper, A. B. (1985) *Biochim. Biophys. Acta* **827,** 320–326
16. Endo, K., Hayashi, Y., Hibi, T., Hosono, K., Beppu, T., and Ueda, K. (2003) *J. Biochem.* **133,** 671–677
17. Machczynski, M. C., Vijgenboom, E., Samyn, B., and Canters, G. W. (2004) *Protein Sci.* **13,** 2388–2397
18. Niladevi, K. N., Jacob, N., and Prema, P. (2008) *Process Biochem.* **43,** 654–660
19. Skálová, T., Dohnálek, J., Østergaard, L. H., Østergaard, P. R., Kolenko, P., Dusková, J., Stepánková, A., and Hasek, J. (2009) *J. Mol. Biol.* **385,** 1165–1178
20. Hyman, M. R., and Arp, D. J. (1992) *J. Biol. Chem.* **267,** 1534–1545
21. Stein, L. Y., and Arp, D. J. (1998) *Appl. Environ. Microbiol.* **64,** 1514–1521
22. Bourbonnais, R., Paice, M. G., Reid, I. D., Lanthier, P., and Yaguchi, M. (1995) *Appl. Environ. Microbiol.* **61,** 1876–1880
23. Otwinowski, Z., and Minor, W. (1997) *Methods Enzymol.* **276,** 307–326
24. Vonrhein, C., Blanc, E., Roversi, P., and Bricogne, G. (2007) in *Methods in Molecular Biology* (Doublié, S., ed) pp. 215–230, Humana Press, Inc., Totowa, NJ
25. Emsley, P., and Cowtan, K. (2004) *Acta Crystallogr. Sect. D Biol. Crystallogr.* **60**, 2126–2132
26. Morris, R. J., Perrakis, A., and Lamzin, V. S. (2003) *Methods Enzymol.* **374,** 229–244
27. Murshudov, G. N., Vagin, A. A., and Dodson, E. J. (1997) *Acta Crystallogr. Sect. D Biol. Crystallogr.* **53**, 240–255
28. Laskowski, R. A. (1993) *J. Appl. Crystallogr.* **26,** 283–291
29. DeLano, W. L. (2002) *The PyMOL Molecular Graphics System*, DeLano Scientific, Palo Alto, CA
30. Poirot, O., O'Toole, E., and Notredame, C. (2003) *Nucleic Acids Res.* **31,** 3503–3506
31. Poirot, O., Suhre, K., Abergel, C., O'Toole, E., and Notredame, C. (2004) *Nucleic Acids Res.* **32,** W37-W40
32. Krissinel, E., and Henrick, K. (2004) *Acta Crystallogr. Sect. D Biol. Crystallogr.* **60**, 2256–2268
33. Collaborative Computational Project, Number 4 (1994) *Acta Crystallogr. Sect. D Biol. Crystallogr.* **50**, 760–763
34. Sippl, M. J. (2008) *Bioinformatics (Oxf.)* **24,** 872–873
35. Sippl, M. J., and Wiederstein, M. (2008) *Bioinformatics (Oxf.)* **24,** 426–427
36. Adman, E. T., Godden, J. W., and Turley, S. (1995) *J. Biol. Chem.* **270,** 27458–27474
37. Kukimoto, M., Nishiyama, M., Ohnuki, T., Turley, S., Adman, E. T., Horinouchi, S., and Beppu, T. (1995) *Protein Eng.* **8,** 153–158
38. Kukimoto, M., Nishiyama, M., Tanokura, M., Adman, E. T., and Horinouchi, S. (1996) *J. Biol. Chem.* **271,** 13680–13683
39. Murphy, L. M., Dodd, F. E., Yousafzai, F. K., Eady, R. R., and Hasnain, S. S. (2002) *J. Mol. Biol.* **315,** 859–871
40. Kukimoto, M., Nishiyama, M., Murphy, M. E., Turley, S., Adman, E. T., Horinouchi, S., and Beppu, T. (1994) *Biochemistry* **33,** 5246–5252
41. Murphy, M. E., Turley, S., and Adman, E. T. (1997) *J. Biol. Chem.* **272,** 28455–28460
42. Inoue, T., Gotowda, M., Deligeer, Kataoka, K., Yamaguchi, K., Suzuki, S., Watanabe, H., Gohow, M., and Kai, Y. (1998) *J. Biochem.* **124,** 876–879
43. Boulanger, M. J., and Murphy, M. E. (2002) *J. Mol. Biol.* **315,** 1111–1127
44. Murphy, M. E. P., Turley, S., Kukimoto, M., Nishiyama, M., Horinouchi, S., Sasaki, H., Tanokura, M., and Adman, E. T. (1995) *Biochemistry* **34,** 12107–12117
45. Garavaglia, S., Cambria, M. T., Miglio, M., Ragusa, S., Iacobazzi, V., Palmieri, F., D'Ambrosio, C., Scaloni, A., and Rizzi, M. (2004) *J. Mol. Biol.* **342,** 1519–1531
46. Bento, I., Martins, L. O., Lopes, G. G., Arménia Carrondo, M., and Lindley, P. F. (2005) *Dalton Trans.* **21,** 3507–3513
47. Lyashenko, A. V., Bento, I., Zaitsev, V. N., Zhukhlistova, N. E., Zhukova, Y. N., Gabdoulkhakov, A. G., Morgunova, F. Y., Voelter, W., Kachalova, G. S., Stepanova, E. V., Koroleva, G. V., Lamzin, V. S., Tishkov, V. I., Betzel, C., Lindley, P. F., and Mikhailov, A. M. (2006) *J. Biol. Inorg. Chem.* **11,** 963–973
48. Zhukova, Y. N., Zhukhlistova, N. E., Lyashenko, A. V., Morgunova, E. Y., Zaitsev, V. N., and Mikhailov, A. M. (2007) *Crystallogr. Rep.* **52,** 826–837
49. Ducros, V., Brzozowski, A. M., Wilson, K. S., Brown, S. H., Østergaard, P., Schneider, P., Yaver, D. S., Pederson, A. H., and Davies, G. J. (1998) *Nat. Struct. Biol.* **5,** 310–316
50. Messerschmidt, A., Luecke, H., and Huber, R. (1993) *J. Mol. Biol.* **230,** 997–1014
51. Corbett, M. C., Latimer, M. J., Poulos, T. L., Sevrioukova, I. F., Hodgson, K. O., and Hedman, B. (2007) *Acta Crystallogr. Sect. D Biol. Crystallogr.* **63**, 951–960
52. Sommerhalter, M., Lieberman, R. L., and Rosenzweig, A. C. (2005) *Inorg. Chem.* **44,** 770–778
53. Yano, J., Kern, J., Irrgang, K. D., Latimer, M. J., Bergmann, U., Glatzel, P., Pushkar, Y., Biesiadka, J., Loll, B., Sauer, K., Messinger, J., Zouni, A., and Yachandra, V. K. (2005) *Proc. Natl. Acad. Sci. U. S. A.* **102,** 12047–12052
54. Ferraroni, M., Myasoedova, N. M., Schmatchenko, V., Leontievsky, A. A., Golovleva, L. A., Scozzafava, A., and Briganti, F. (2007) *BMC Struct. Biol.* **7,** 60
55. Durao, P., Chen, Z., Fernandes, A. T., Hildebrandt, P., Murgida, D. H., Todorovic, S., Pereira, M. M., Melo, E. P., and Martins, L. O. (2008) *J. Biol. Inorg. Chem.* **13,** 183–193
56. Galli, I., Musci, G., and Bonaccorsi di Patti, M. C. (2004) *J. Biol. Inorg. Chem.* **9,** 90–95
57. Roberts, S. A., Weichsel, A., Grass, G., Thakali, K., Hazzard, J. T., Tollin, G., Rensing, C., and Montfort, W. R. (2002) *Proc. Natl. Acad. Sci. U. S. A.* **99,** 2766–2771
58. Ellis, M. J., Grossmann, J. G., Eady, R. R., and Hasnain, S. S. (2007) *J. Biol. Inorg. Chem.* **12,** 1119–1127